TABLE I
FIELD LEVELS IN WR10 AND WR90

E(MV/m)	P(W) - WR10
0.8	1.00E+03
2.5	1.00E+04
7.8	1.00E+05
24.7	1.00E+06

E(MV/m)	P(W) - WR90
0.9	1.00E+05
2.8	1.00E+06
8.9	1.00E+07
28.1	1.00E+08

ACKNOWLEDGMENT

The authors would like to thank O. Millican, Stanford Linear Accelerator Center (SLAC), Stanford, CA, and D. Shelly, SLAC, for their expert assistance in fabrication of the phase shifter.

REFERENCES

[1] C. Adolphsen *et al.*, "RF processing of X-band accelerator structures at the NLCTA," in *Proc. 20th Int. Linac Conf.*, Monterey, CA, Aug. 2000, SLAC-PUB-8573, pp. 21–25.
[2] D. H. Whittum, "Ultimate gradient in solid-state accelerators," in *Proc. Advanced Accelerator Concepts Workshop*, 1999, pp. 72–85.
[3] M. E. Hill *et al.*, "Beam-cavity interaction circuit at W-band," *IEEE Trans. Microwave Theory Tech.*, vol. 49, pp. 998–1000, May 2001.
[4] R. E. Green, Ed., *Machinery's Handbook*. New York: Ind. Press, 1996, p. 239.

An Inverse Scattering Technique for Microwave Imaging of Binary Objects

Ioannis T. Rekanos and Theodoros D. Tsiboukis

***Abstract*—In this paper, an inverse scattering method for detecting the location and estimating the shape of two-dimensional homogeneous scatterers is presented. It is assumed that the permittivity and conductivity of the scatterer are given. Thus, the method concentrates on reconstructing the domain occupied by the scatterer. The inversion is based on scattered electric far-field measurements and is carried out by a combined finite-element–nonlinear optimization technique. The computational burden is reduced by use of the adjoint-state-vector methodology. Finally, the proposed method is applied to both penetrable and impenetrable scatterers.**

***Index Terms*—Finite-element methods, gradient methods, image reconstruction, inverse scattering, microwave imaging.**

I. INTRODUCTION

In most cases concerning electromagnetic inverse scattering, the objective is to reconstruct the distribution of the constitutive parameters of a specimen using scattered-field measurements. A specific type of this problem consists in estimating the location and shape of a scatterer that has known electromagnetic properties [1]–[3]. In this case, we deal with a binary object reconstruction problem and our aim is to identify the presence or the absence of the scatterer at specified subsections of the domain under investigation. This approach is a very useful tool for nondestructive testing applications [1] and is appropriate for applications where physical limitations do not allow explicit and quantitative reconstruction [2], [3].

The purpose of this paper is to extend the inverse scattering method proposed in [4] to the case of binary objects. As in its initial form, the method combines the finite-element method (FEM) [5] and the Polak–Ribière nonlinear-conjugate-gradient (NCG) optimization algorithm [6]. Its objective is to minimize an error function that represents the difference between the estimated and measured scattered electric far field. The parameters that describe the scatterer are Boolean variables since they refer to its presence or absence. Hence, the error function has to be modified to a differentiable form in order to compute its gradient. After an appropriate modification [1], the gradient is computed by an FEM-based sensitivity-analysis scheme [7], which is enhanced by the adjoint-state-vector methodology (ASVM) [6]. In numerical results, the proposed method is applied to the reconstruction of penetrable and impenetrable scatterers, while the case of noisy measurements is also examined.

II. DIRECT PROBLEM

We consider an infinitely long, isotropic, and nonmagnetic cylindrical scatterer of bounded cross-section S, which is uniform along the z-axis. It is assumed that the scatterer has constant and known permittivity ε_s and conductivity σ_s and is embedded in a homogeneous medium $(\varepsilon_b, \sigma_b)$. For a given excitation frequency ω, the scatterer is represented by the complex permittivity contrast (CPC) given by

$$\chi(x, y) = \left[\left(\varepsilon_s - j\frac{\sigma_s}{\omega}\right)\Big/\left(\varepsilon_b - j\frac{\sigma_b}{\omega}\right) - 1\right]u(x, y) = \chi_s u(x, y). \tag{1}$$

The function $u(x, y)$ is called *function of support*, and is equal to one or zero when the point (x, y) lies inside or outside S, respectively. If the scatterer is illuminated by a TM-polarized incident wave, then the scattered electric field satisfies the scalar Helmholtz equation. As in [4], we compute the field by applying the FEM, which results in the sparse system of equations

$$\mathbf{S}(\mathbf{u})\mathbf{E} = \mathbf{b}\left(\mathbf{u}, \mathbf{E}^{\mathrm{inc}}\right) \tag{2}$$

where the vectors $\mathbf{E}$ and $\mathbf{E}^{\mathrm{inc}}$ represent the scattered and incident field values at the nodes of the mesh. Both matrices $\mathbf{S}$ and $\mathbf{b}$ depend on the binary vector $\mathbf{u} = [u_1\, u_2\, \cdots\, u_M]^T$, where u_m is the constant value of $u(x, y)$ inside the mth element, and M is the total number of elements. After the solution of (2), we calculate the scattered far field by applying the Helmholtz–Kirchhoff integral theorem. In particular, the calculation of the far field at K positions can be represented by the matrix form

$$\mathbf{E}^f = \left[E_1^f\, E_2^f \cdots E_K^f\right]^T = \mathbf{Q}\mathbf{E} \tag{3}$$

where $\mathbf{Q}$ is a sparse matrix associated with the Green's function and its derivative.

Manuscript received August 19, 1999; revised October 18, 2000.

I. T. Rekanos was with the Division of Telecommunications, Department of Electrical and Computer Engineering, Aristotle University of Thessaloniki, Thessaloniki 54004, Greece. He is now with the Radio Laboratory, Helsinki University of Technology, Espoo, FIN 02015 HUT, Finland (e-mail: rekanos@cc.hut.fi).

T. D. Tsiboukis is with the Division of Telecommunications, Department of Electrical and Computer Engineering, Aristotle University of Thessaloniki, Thessaloniki 54006, Greece (e-mail: tsibukis@vergina.eng.auth.gr).

Publisher Item Identifier S 0018-9480(02)04043-7.

III. Inversion

The scatterer profile is reconstructed from scattered far-field measurements taken around the scatterer domain. For I incidences and K measurement positions, we obtain a set of vectors $\mathbf{f}_i = [f_{i1}\, f_{i2} \cdots f_{iK}]^T$, $(1 \le i \le I)$, where f_{ik} is the measurement at the kth position for the ith incidence. We then reconstruct the scatterer profile $\mathbf{u}$ by minimizing the error function

$$F(\mathbf{u}) = I^{-1} \sum_{i=1}^{I} |\mathbf{f}_i|^{-2} |\mathbf{f}_i - \mathbf{Q}\mathbf{E}_i|^2 \tag{4}$$

where $\mathbf{E}_i$ is the FEM solution for the ith incidence. Since $\mathbf{u}$ is binary, the error function (4) is not differentiable. To overcome this limitation, we modify the function of support, i.e., $u[w(x, y)] = 1/\{1 + \exp[-w(x, y)/\theta]\}$, where the positive parameter θ controls the steepness of u [1]. Thus, the mth element is occupied by the scatterer when $w_m > 0$. This modification allows us to minimize (4) by applying the Polak–Ribière NCG algorithm. The computation of the gradient of the error function with respect to the vector $\mathbf{w}$, $(u_m = u(w_m))$ requires the solution of M systems of equations for each incidence. As reported in [4], we can reduce the computation time by applying the ASVM. Thus, for each incidence, we solve only the system

$$\mathbf{S}\mathbf{g}_i = -2\mathbf{Q}^T (\mathbf{f}_i - \mathbf{Q}\mathbf{E}_i)^*. \tag{5}$$

The gradient of F is then given by

$$\partial_{\mathbf{w}} F = I^{-1} \sum_{i=1}^{I} |\mathbf{f}_i|^{-2} \mathrm{Re}\left\{ \left[\partial \mathbf{b}_i / \partial \mathbf{w} - (\partial \mathbf{S} / \partial \mathbf{w}) \mathbf{E}_i \right]^T \mathbf{g}_i \right\}. \tag{6}$$

Furthermore, since $\mathbf{S}$ is the same for all incidences, we decompose it once during each iteration by applying the Cholesky factorization.

The main advantage of applying the FEM to inverse scattering problems is that the resulting systems of equations are sparse. Consequently, the time and storage demands are lower compared to the method of moments (MoM), which has been used in previous studies. In addition, by applying the ASVM, the computational burden can be drastically reduced. Moreover, the near-to-far-field transformation is also rapidly achieved by a sparse-matrix multiplication. Another characteristic of the FEM is that we can satisfy the continuity of the tangential component of the field along the borders of the cells by using edge elements. In our case, since the unknown field is TM polarized, the tangential continuity is satisfied even by using nodal elements. On the contrary, by applying the MoM, the tangential-field component along the borders of cells is discontinuous. Apart from the different modeling approach (FEM versus MoM), the presented method has another difference compared to the modified-gradient technique [1]. Here, the direct scattering problem is solved during each iteration, while in [1], it is not solved at all. However, in the modified-gradient technique, the number of iterations required to achieve reconstruction is much higher.

IV. Numerical Results

The proposed inverse-scattering method has been applied to the reconstruction of the location and shape of either penetrable and lossy or impenetrable scatterers. It is assumed that the scatterer lies within a known square domain of interest. Furthermore, we have the *a priori* knowledge of the CPC value χ_s. In each application, synthetic measurements, which are obtained by solving the direct-scattering problem, are used. Actually, we have simulated the measurements by applying the FEM. The fact that the FEM is also used for modeling the inverse problem could lead to good reconstruction results, which are not representative (known as "inverse crime"). For this reason, the mesh that is used for simulating the measurements is different from the one used during the inversion, and is actually more dense. Also, we examine the reliability of the method, by inverting noisy measurements. We note that, in the following examples, the initial value of the function of support is 0.05 (a selection almost equivalent to the absence of the scatterer).

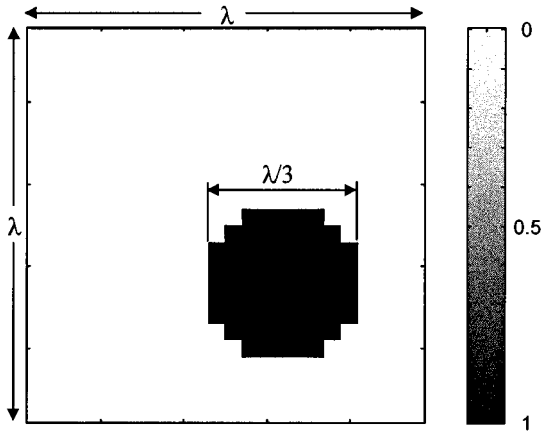

Fig. 1. Profile of a conducting scatterer. The original function of support.

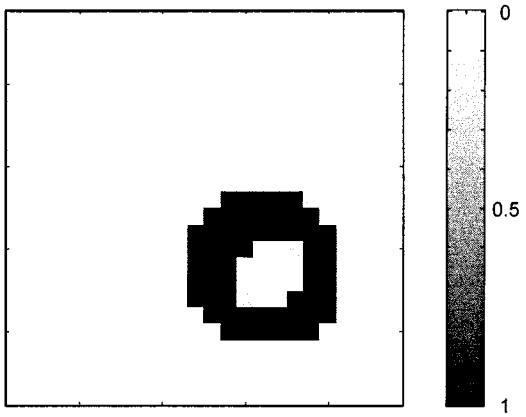

Fig. 2. Reconstructed function of support of the conducting scatterer for $\chi_s = -j40$.

A. Impenetrable Scatterer

In the first example, a conducting scatterer of circular cross section, which is embedded in free space, is considered (Fig. 1). Its diameter is equal to $\lambda/3$, where λ is the wavelength of the excitation in free space. The domain of interest, which contains the scatterer, is square of side equal to λ. First, the scatterer is illuminated by TM plane waves from 30 directions around the domain of interest. For each incidence, the scattered electric far field is measured at 30 positions uniformly distributed around the domain of interest on a circle of radius equal to 8λ. The domain of interest is divided into 24×24 square subsections, while each subsection is assumed to have constant CPC. Thus, the scatterer profile is described by a vector that has 576 unknown components.

Before the inversion begins, the known value of the CPC has to be set. As shown in [3], the value of χ_s should be set such that the boundary of the scatterer is reconstructed with a thickness of two or three times the mesh width. In this application, it is found that $\chi_s = -j\,40$ satisfies the above condition. After 16 iterations, there was no essential further reduction of the error function. The reconstructed profile is shown in Fig. 2. It is clear that both the location and boundary of the scatterer have been successfully estimated. Furthermore, the interior of the object has not been reconstructed. This is an expected result since a conducting scatterer is indistinguishable from a conducting shell of

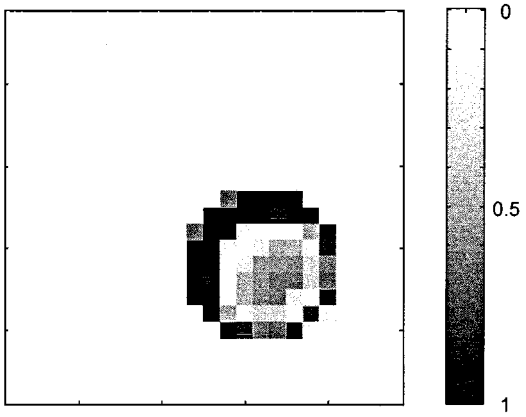

Fig. 3. Reconstructed function of support of the conducting scatterer for $\chi_s = -j150$.

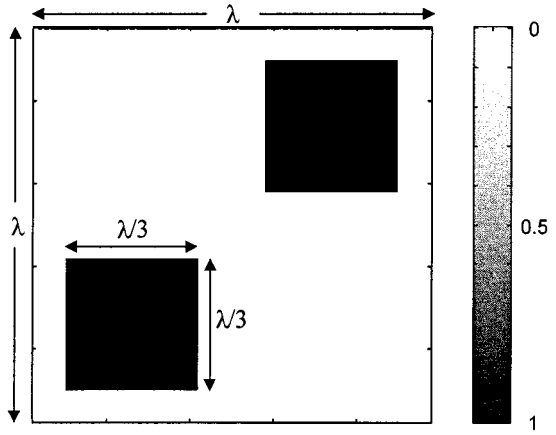

Fig. 4. Profile of two distinct penetrable scatterers ($\chi_s = 0.8 - j0.6$). The original function of support.

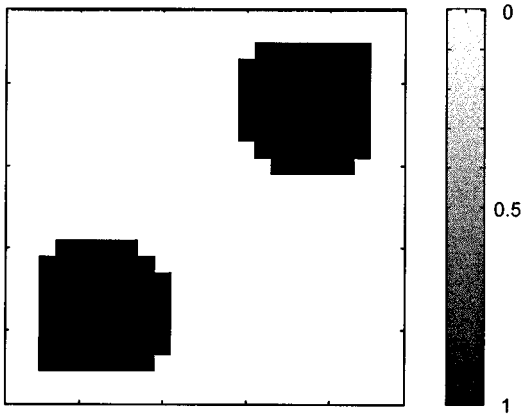

Fig. 5. Reconstructed function of support of the two distinct penetrable scatterers based on noiseless measurements.

the same shape. If we set $\chi_s = -j150$, the corresponding penetration depth is less than the mesh width, resulting in a highly oscillatory function of support (Fig. 3).

B. Distinct Penetrable Lossy Scatterers

In the second example, we consider two lossy and homogeneous scatterers of $\lambda/3 \times \lambda/3$ square cross section each (Fig. 4). The CPC of both scatterers is $\chi_s = 0.8 - j0.6$. The entire structure lies within a $\lambda \times \lambda$ square domain divided into 24×24 square subdivisions. As in the first example, the scatterers are illuminated from 30 directions, while 30 measurements are obtained for each incidence. The reconstructed function of support, after 16 iterations, is illustrated in Fig. 5. We notice that limited errors appear in the domain between the two scatterers because of their interaction.

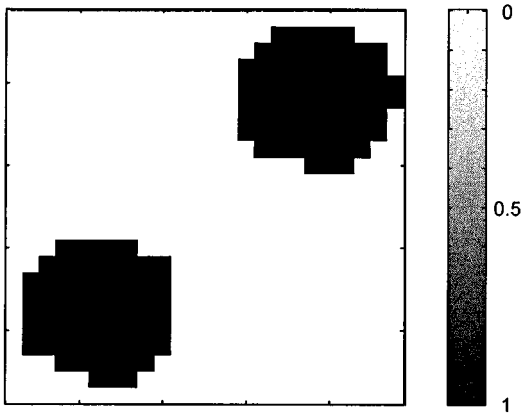

Fig. 6. Reconstructed function of support of the two distinct penetrable scatterers based on noisy measurements ($\mathrm{SNR} = 10$ dB).

To examine the efficiency of the method in the presence of noise, we apply it to noisy data. These data are generated by adding white Gaussian noise of 10-dB signal-to-noise ratio to noiseless measurements. As shown in Fig. 6, the reconstructed profile proves the applicability of the method to the case of noisy data. This reliability could be attributed to the *a priori* knowledge of the CPC value, which reduces the dimension of the solution space and acts as a regularization scheme.

V. Conclusions

A spatial-domain inverse-scattering method has been presented for the reconstruction of the location and shape of scatterers that have known electromagnetic properties. By modifying the binary function of scatterer support, we are able to use an optimization scheme combining the FEM and Polak–Ribière NCG algorithm. The application of the method to both penetrable and impenetrable scatterers was successful, even in the presence of noisy measurements.

References

[1] L. Souriau, B. Duchêne, D. Lesselier, and R. E. Kleinman, "Modified gradient approach to inverse scattering for binary objects in stratified media," *Inv. Problems*, vol. 12, no. 4, pp. 463–481, Aug. 1996.

[2] H. Belkebir, R. E. Kleinman, and C. Pichot, "Microwave imaging—Location and shape reconstruction from multifrequency scattering data," *IEEE Trans. Microwave Theory Tech.*, vol. 45, pp. 469–476, Apr. 1997.

[3] R. E. Kleinman and P. M. van den Berg, "Two-dimensional location and shape reconstruction," *Radio Sci.*, vol. 29, no. 4, pp. 1157–1169, July–Aug. 1994.

[4] I. T. Rekanos, T. V. Yioultsis, and T. D. Tsiboukis, "Inverse scattering using the finite-element method and a nonlinear optimization technique," *IEEE Trans. Microwave Theory Tech.*, vol. 47, pp. 336–344, Mar. 1999.

[5] J. Jin, *The Finite Element Method in Electromagnetics*. New York: Wiley, 1993.

[6] P. Neittaanmäki, M. Rudnicki, and A. Savini, "Inverse problems and optimal design in electricity and magnetism," in *Monographs in Electrical and Electronic Engineering 35*. Oxford, U.K.: Clarendon, 1996.

[7] S. Gitosusastro, J. L. Coulomb, and J. C. Sabonnadiere, "Performance derivative calculations and optimization process," *IEEE Trans. Magn.*, vol. 25, pp. 2834–2839, July 1989.